

Substitution, dimerization, metalation, and ring-opening reactions of *N*-fused porphyrins

Tomoya Ishizuka^{a,b}, Shinya Ikeda^a, Motoki Toganoh^a, Ichiro Yoshida^c,
Yuichi Ishikawa^c, Atsuhiko Osuka^b, Hiroyuki Furuta^{a,b,*}

^a Department of Chemistry and Biochemistry, Graduate School of Engineering, Kyushu University, Fukuoka 819-0395, Japan

^b Department of Chemistry, Graduate School of Science, Kyoto University, Kyoto 606-8502, Japan

^c Department of Applied Chemistry, Faculty of Engineering, Oita University, Oita 870-1124, Japan

Received 15 January 2008; received in revised form 12 February 2008; accepted 13 February 2008

Available online 16 February 2008

Abstract

A variety of reactions such as substitution, dimerization, rhenium(I) metalation, and ring-opening reactions of *N*-fused porphyrin (NFP) and optical properties of the products are presented. Palladium-catalyzed cross-coupling reactions under Suzuki or Stille conditions afford aryl and aryloxy-substituted NFPs (**12**, **14**) and an ethynyl-bridged dimer (**15**) from 3-bromo-substituted NFP (**3b**) in 40–98% yields. Treatment of NFP with silver(I) trifluoroacetate in CHCl₃ affords a dimer (**22**) linked at both C21-positions of the fused rings and its bis-Re(I) metal complex (**24**) is synthesized. X-ray structures of the 3-trifluoromethyl and 3-phenyl NFP derivatives (**9e** and **12a**) reveal the three-center hydrogen bondings in the core. All the new NFP derivatives display unique absorption spectra, and particularly, ethyne-bridged NFP-dimer (**15**) shows a remarkable bathochromic shift into a near-infrared region showing an absorption band at 1020 nm with tailing up to 1100 nm. Moreover, alkoxide nucleophiles convert NFP into NCP derivatives by the cleavage of C–N bond in the fused ring, which is useful for the preparation of various C3-substituted NCPs and C21,C21'-linked NCP dimers from NFPs.

© 2008 Elsevier Ltd. All rights reserved.

Keywords: *N*-Fused porphyrin; Pd-catalyzed cross-coupling; Dimerization; Re(I) complexes

1. Introduction

Porphyrin (**1**) and its analogues have gained much attention due to their interesting optical, electrochemical, and coordination properties with potential for functional molecules in the application fields.^{1,2} Among various porphyrin analogues, *N*-confused porphyrin (NCP, **2**)^{3,4} is unique in that it transforms into another class of porphyrinoid, *N*-fused porphyrin (NFP, **3**).^{5,6} The examples of such porphyrinoids bearing one or two [5.5.5] fused tri-pentacyclic rings are rather limited but gradually accumulating, especially, in the tetra- and pentapyrrolic macrocycle systems. For examples, trans-doubly *N*-confused porphyrin was reported to be synthesized from doubly *N*-confused, *N*-fused porphyrin (NC₂FP, **4**) via ring-

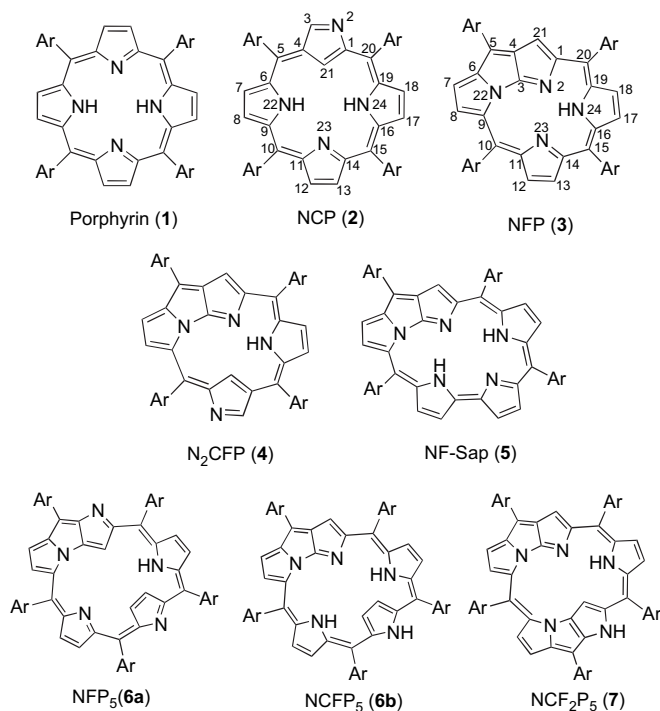
opening reaction.⁷ In the pentapyrrolic system, *N*-fused sapphyrin (NF-Sap, **5**) was obtainable from *N*-confused sapphyrin with a similar reaction used for NFP.⁸ Moreover, *N*-fused pentaphyrin (NFP₅, **6a**) and *N*-confused, *N*-fused pentaphyrin (NCFP₅, **6b**) were synthesized and their Rh(I) coordination chemistry was investigated.^{9,10} The latter **6b** is shown to transform into doubly fused pentaphyrin (N₂FP₅, **7**).^{10a} The interconversion between *N*-confused porphyrins and *N*-fused porphyrins is one of the characteristic features of these porphyrinoids.

The properties of NFP are also characteristic. For example, in spite of its 18π aromatic system same as standard porphyrin, NFP displays absorption in a near-infrared region and the edge exceeds over 1000 nm.⁵ The coordination chemistry of NFP is of particular interest since NFP could serve as a monovalent 6-electron donor ligand, which is isoelectronic as cyclopentadienyl anion (Cp) and hydrotris(1-pyrazoyl)borate (Tp)

* Corresponding author. Tel./fax: +81 92 802 2865.

E-mail address: hfuruta@cstf.kyushu-u.ac.jp (H. Furuta).

Chart 1.



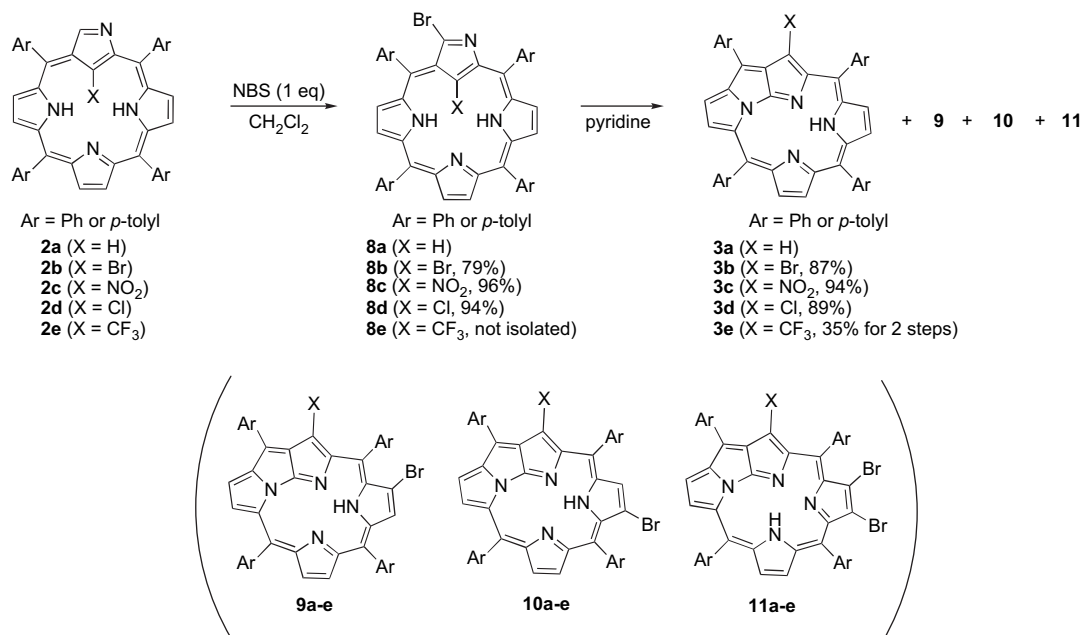
ligands.⁶ So far, only rhenium^{6a–e} and boron^{6f} metal complexes have been reported and the Re(VII)-trioxo complexes are revealed to catalyze deoxygenation reactions of *N*-oxides with high efficiency.^{6c} Stimulated by these findings, the investigation of NFP chemistry is now rapidly progressing. Herein, we report the fundamental reactivity of NFP for substitution, Pd-catalyzed cross-coupling, dimerization, Re(I) metalation, and ring-opening reactions. In addition, the optical absorption properties of various NFP derivatives are presented.

2. Results and discussion

2.1. *N*-Fused porphyrin from *N*-confused porphyrin

As previously reported,⁵ treatment of 21-substituted NCP (**2**) with 1 equiv of *N*-bromosuccinimide (NBS) in CH₂Cl₂ affords 3-bromo NCP **8** (Scheme 1). Compound **8** is relatively unstable in solution, and in pyridine, it gradually changes into 21-substituted NFP **3** in high yields (80–95%). In this reaction, the confused pyrrole ring flips and forms a new bond between C3 and N22 atoms with elimination of an HBr molecule, affording a fused tri-pentacyclic ring. Consequently, reflecting the high reactivity of adjacent β-pyrrolic carbons (C17, C18) in **3**, brominated NFP derivatives **9–11** were obtained as byproducts. Monobrominated NFP isomers **9** and **10** were difficult to separate by column chromatography because of the similar polarity. In the case of **3e** (Ar=phenyl), however, the second bromination occurs only at C18-position to afford **9e**, selectively. Further bromination of **9e** hardly proceeds and thus, only a trace amount of dibrominated **11e** was obtained. The detail mechanism of this selective bromination of **3e** is not clear, but the strong electron-withdrawing trifluoromethyl group at C21-position decreases the reactivity for electrophilic substitution. In fact, **3c** with a stronger electron-withdrawing nitro group at C21-position is almost inactive for the peripheral bromination.

The structure of **9e** was confirmed by X-ray diffraction analysis (Fig. 1). The NFP core is almost planar and a mean deviation of the porphyrin core is 0.164 Å. A trifluoromethyl group and a bromine atom are attached at C21- and C18-positions, respectively. The N(4)-containing pyrrolic ring is tilted by 5.58° to the least-square plane consisting of the core 24 atoms, due to the steric repulsion between Br and the neighboring 20-phenyl group. The characteristic



Scheme 1.

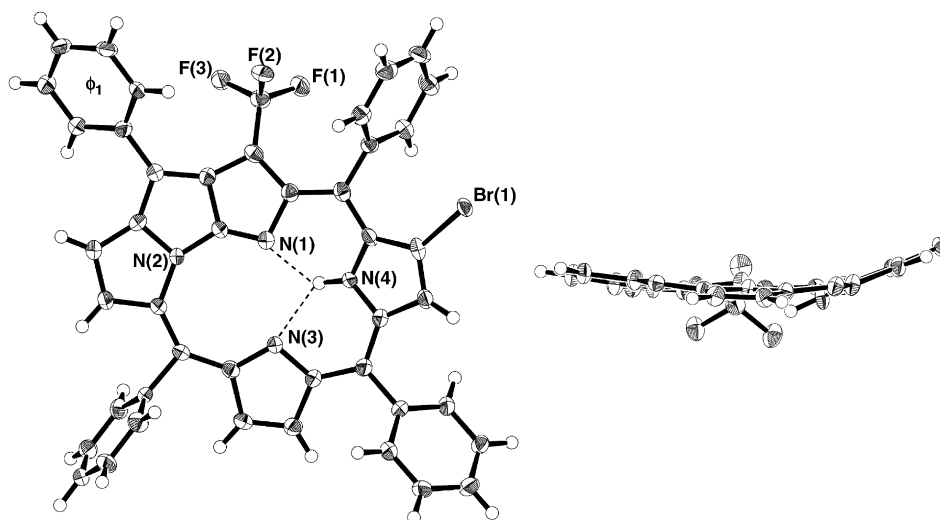
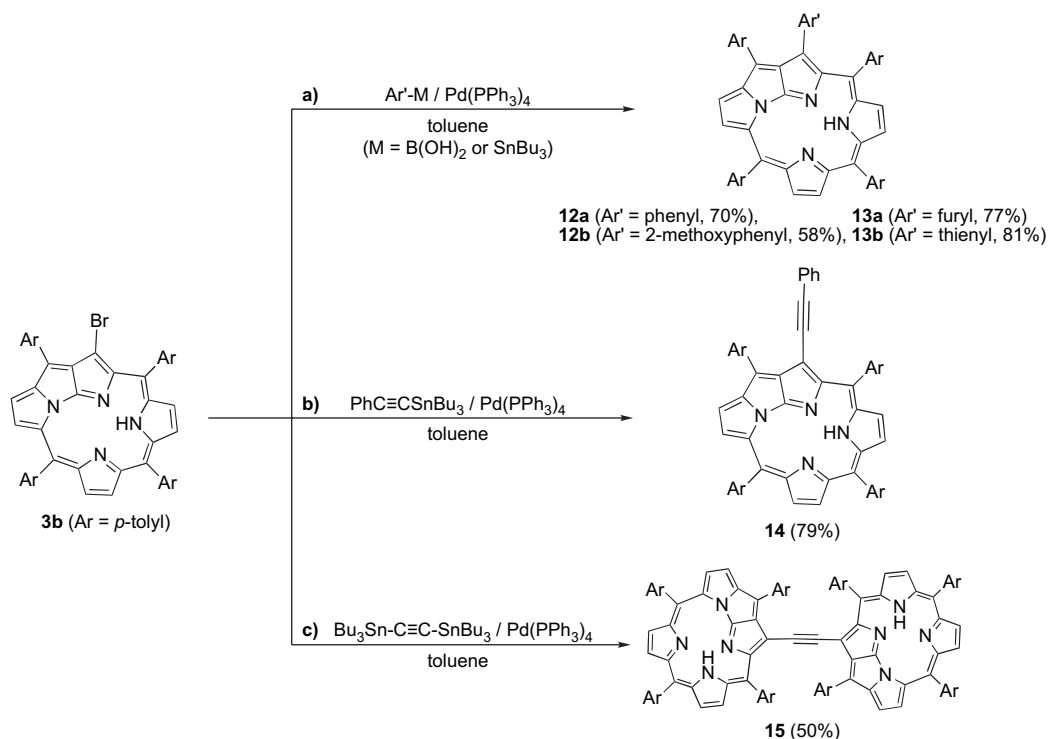


Figure 1. X-ray structure of **9e**. Top view (left) and side view (right). *meso*-Phenyl groups are omitted for clarity in the side view.

short inter atomic distances between the core three nitrogen atoms, N(1), N(3), and N(4), are preserved: 2.860 (5), 2.525 (2), and 2.677 (5) Å for N(1)⋯N(3), N(1)⋯N(4), and N(3)⋯N(4), respectively, which allow strong hydrogen bondings between inner hydrogen (NH) and three nitrogen atoms in the core.⁵ Actually, the NH signal is largely shifted to an unusual lower field and observed at 6.12 ppm, indicating the inner-core hydrogen bondings. The peculiar coplanarity between the 5-phenyl group (ϕ_1) and the NFP core plane is slightly lost in **9e** due to the neighboring bulky 21-trifluoromethyl group, showing the dihedral angle of 31.35° (vs 12.4° for **3a**).^{5b} The deviation from the

coplanarity makes the bond length between the phenyl (ϕ_1) carbon and *meso*-C5 atom a little longer (1.472(6) Å) than that of **3a** (1.438(7) Å), which is in the average bond length of nonconjugated C(sp²)–C(sp²) single bonds (1.47–1.48 Å).¹¹

18,19-Dibromo NFP **11** can be also synthesized quantitatively, from the reaction of **3** with 2 equiv of NBS or using a mixture of **9** and **10** with 1 equiv of NBS. In NFP **3**, the inner hydrogen (NH) is connected to N(4), whereas in **11**, the hydrogen atom is attached at N(3), probably because of the enhanced acidity of N(4)-containing pyrrole moiety due to the bromo groups directly attached.



Scheme 2.

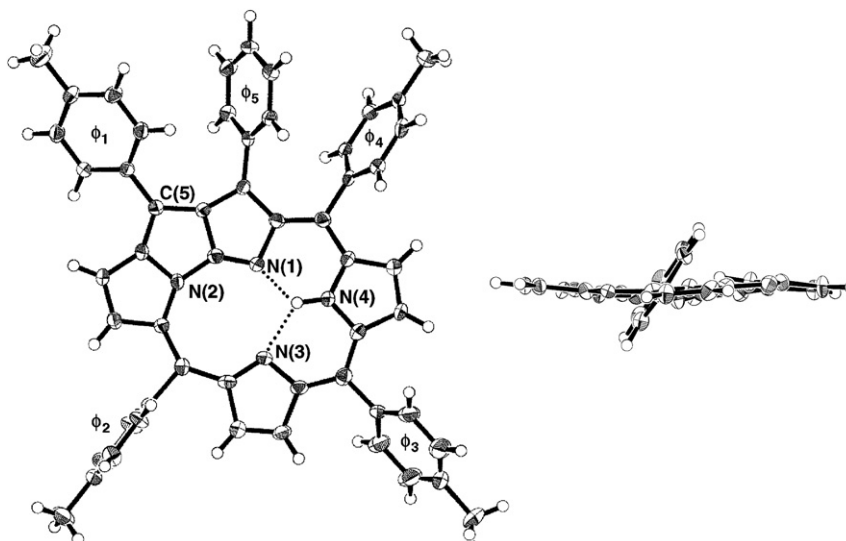


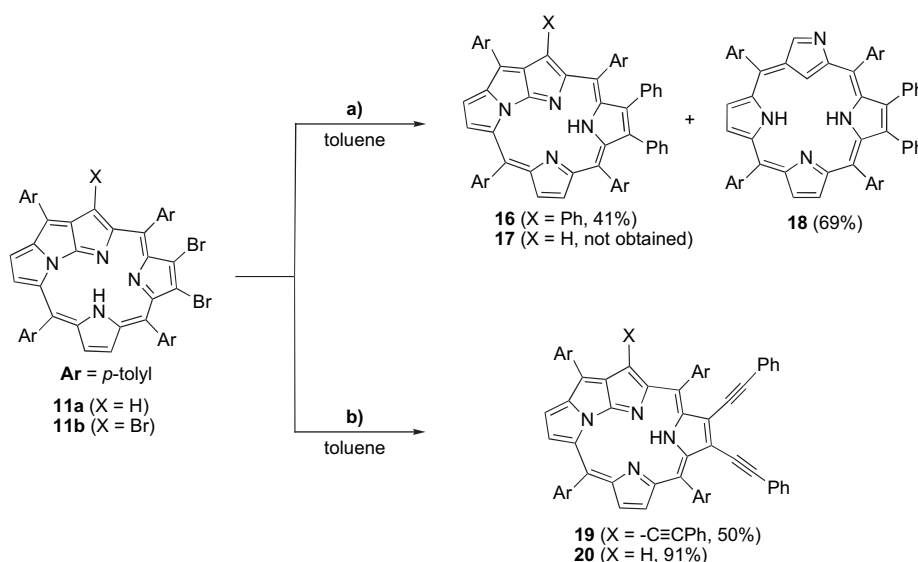
Figure 2. X-ray structure of **12a**. Top view (left) and side view (right). *meso*-Tolyl groups are omitted for clarity in the side view.

2.2. Palladium coupling of 21-bromo NFP

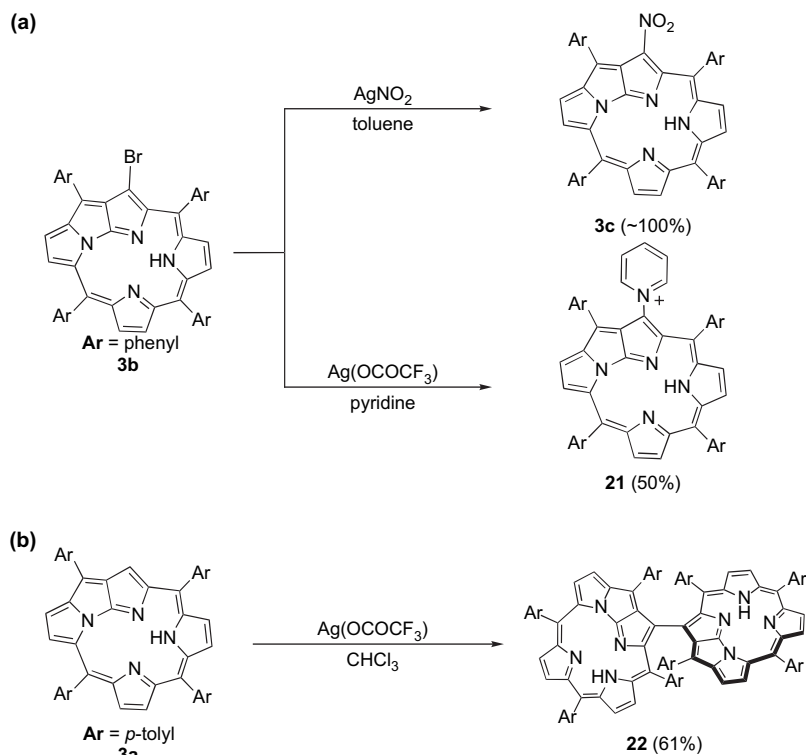
The 21-bromo group at the fused ring of **3b** is reactive for the cross-coupling reactions by palladium catalysts.^{12–14} Under Suzuki coupling conditions with phenylboronic acid and 2-methoxyphenylboronic acid, 21-aryl-substituted NFP **12a** and **12b** were obtained in 70 and 58% yields, respectively (Scheme 2a). In the ¹H NMR spectrum of **12a** in CDCl₃, the introduced phenyl group resonates around 7.0 ppm. The inner NH signal is observed at 8.6 ppm due to the strong hydrogen bondings between the three internal nitrogen atoms. The X-ray structure of **12a** is shown in Figure 2. The phenyl ring (ϕ_5) is located at the C21-position of the fused ring, and the dihedral angle between the porphyrin core plane is 58.92°. The NFP core plane is slightly distorted showing the mean deviation of 0.104 Å, which is comparable to those of **3b** (0.101 Å) and parent NFP (**3a**) (0.127 Å). The distances between the

inner three nitrogen atoms are 2.920(3), 2.495(2), 2.648(2) Å for N(1)⋯N(3), N(1)⋯N(4), and N(3)⋯N(4), respectively, which are short enough to form a three-centered hydrogen bonding. The co-planarity between the 5-tolyl group (ϕ_1) and the NFP core plane is slightly lost similar to **9e**, showing the dihedral angle of 30.82° probably due to the steric repulsion by the 21-phenyl group (ϕ_5). However, the bond length of connecting ϕ_1 carbon and C5 carbon is still short (1.466(3) Å) to maintain the electronic interaction.

Furyl- and thienyl-tributylstannanes also react with **3b** under typical Stille coupling conditions in the presence of Pd(0) catalyst to afford 21-substituted **13a** and **13b** in high yields. However, when a 2,4-disubstituted phenylboronic acid (2,4-dimethoxyphenylboronic acid or pentafluorophenylboronic acid) was employed, corresponding aryl-substituted NFP was not formed, but debromination occurred to afford NFP **3a** quantitatively. Though the detail mechanism is not clear yet,



Scheme 3. (a) PhB(OH)₂/Pd(PPh₃)₄/K₂CO₃; (b) PhC≡CSnBu₃/Pd(PPh₃)₄.



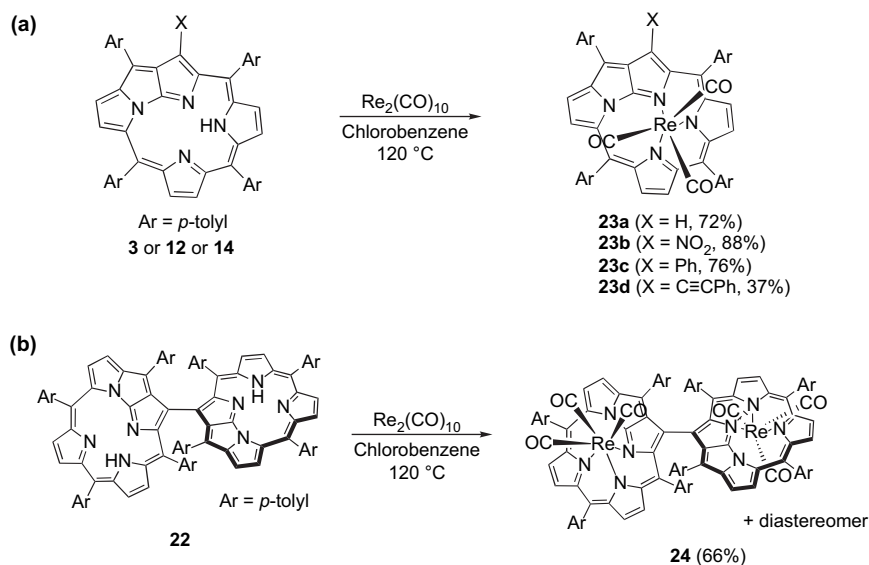
Scheme 4.

the above results suggest that the size of the aryl reagents is significant due to the steric repulsion between the 5,20-*meso*-aryl groups and aryl-substrates in these reactions.

The attempts to introduce arylethynyl substituents at the C21-position of the fused ring under Sonogashira coupling conditions with arylacetylene and catalytic amount of PdCl₂(PPh₃)₂ resulted in the formation of complicated mixture. In the reaction, the divalent palladium metal was probably trapped by the inner nitrogen atoms, which deterred the reaction. Thus, the Stille coupling conditions with tributyl(phenylethy-

nyl)stannane were applied, then the target molecule (**14**) was obtained in 79% yield (Scheme 2b).¹⁵ The inner NH signal is observed at 8.21 ppm and the ¹H signals of phenylethynyl group are observed around 7.2 ppm. The ethynyl sp-carbons appear at 102.6 and 88.5 ppm in the ¹³C NMR spectrum.¹⁴

By employing bis(tributylstannyl)acetylene for the reaction of **3b** in the presence of Pd(PPh₃)₄, 2,2'-ethyne-bridged NFP-dimer (**15**) was obtained in 50% yield (Scheme 2c). Although the X-ray structure of **15** is not yet at hand, the symmetrical structure of the dimer was suggested from the ¹H NMR



Scheme 5.

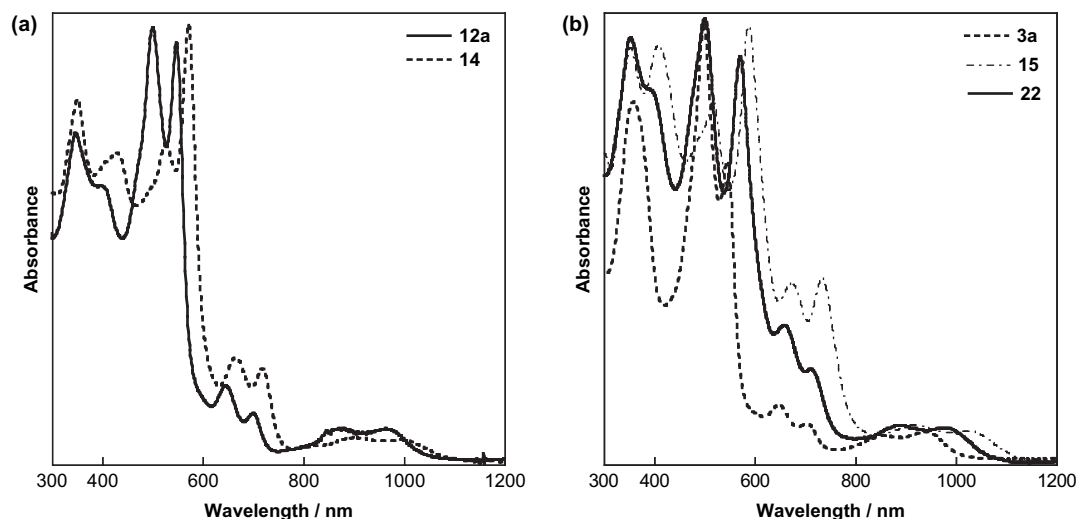


Figure 3. Optical absorption spectra of NFP derivatives (a) **12a**, **14**, and (b) **3a**, **15**, **22** in CH_2Cl_2 .

spectrum in CDCl_3 . In addition, one of the *p*-tolyl groups at *meso*-positions seems to be located above the other NFP plane because one of the methyl signals appears in the higher field at 0.83 ppm due to the ring-current effect. The ethyne-bridge of **15** could assist the electronic communication between the NFP units, judging from the optical absorption (*vide infra*).

To investigate the reactivity of the 18,19-dibromo groups in NFP, the palladium-catalyzed cross-coupling reaction of **11b** ($\text{X}=\text{Br}$) has been performed. Under Suzuki coupling conditions with phenylboronic acid in the presence of $\text{Pd}(\text{PPh}_3)_4$, 18,19,21-triphenyl-substituted NFP (**16**) was obtained in 41% yield (Scheme 3a). The formation of **16** is suggested by the mass spectrum, however, due to the low solubility of **16** in ordinary solvents such as CHCl_3 and toluene, the structural characterization by $^1\text{H NMR}$ remains incomplete. In the reaction with 2,4-dimethoxyphenylboronic acid or pentafluorophenylboronic acid, the introduction of an aryl group at the C21-position in **11b** was also unsuccessful and only C21-debromina

tion took place similarly to **3b** and the 18,19-dibromo groups remain intact during the reactions to afford **11a** in 65–80% yield. Compound **11a** is also susceptible to the cross-coupling reactions. However, the Suzuki coupling reaction with phenylboronic acid did not afford expected 18,19-diphenyl NFP (**17**), but surprisingly, yielded a ring-opening product, 18,19-diphenyl NCP (**18**), in 69% yield. During the reaction, the diphenyl derivative **17** could be formed, but the fused ring might easily undergo bond cleavage to afford **18** (*vide infra*). The $^1\text{H NMR}$ signal of the inner 21-hydrogen in **18** appears at -3.34 ppm and the inner NH signals, which are very broad at room temperature, appear at -1.13 and -1.45 ppm at -40 °C. The signal of the C3-proton is buried in the aryl-group region. The parent MALDI-TOF mass peak of **18** is detected at m/z 822.0 and the optical absorption spectrum displays the Soret band at 454 nm, which are clear evidences of the formation of NCP derivative (**18**). The reformation of NCP from NFP without peripheral 21-substitution is very attractive for the syntheses of various NCP derivatives.

When tribromo NFP (**11b**) and dibromo NFP (**11a**) were treated with tributyl(phenylethynyl)stannane in the presence of $\text{Pd}(\text{PPh}_3)_4$, 18,19,21-triphenylethynyl NFP (**19**) and 18,19-diphenylethynyl NFP (**20**) were obtained in 50 and 91% yield, respectively (Scheme 3b).

2.3. Treatment of NFP with silver(I) salts

When **3b** is treated with silver(I) salts, nucleophilic substitution of the 21-bromo group occurs efficiently. For example, silver(I) nitrite affords 21-nitro-derivative **3c**, quantitatively, in refluxing toluene (Scheme 4a). In this reaction, the substitution may proceed by radical mechanism where the first debromination occurs with the silver(I) ion, then, followed by the reaction of NFP cation radical and a nitrite ion. Partially supporting this, the reaction of **3b** with silver trifluoroacetate in refluxed pyridine afforded 21-(*N*-pyridinium) NFP (**21**) in 52% yield.¹⁶ When the pyridine solvent was replaced by non-nucleophilic solvents like CHCl_3 , the reaction of **3a** yields a self-coupling dimer **22** as reported previously (Scheme 4b).^{5c,17}

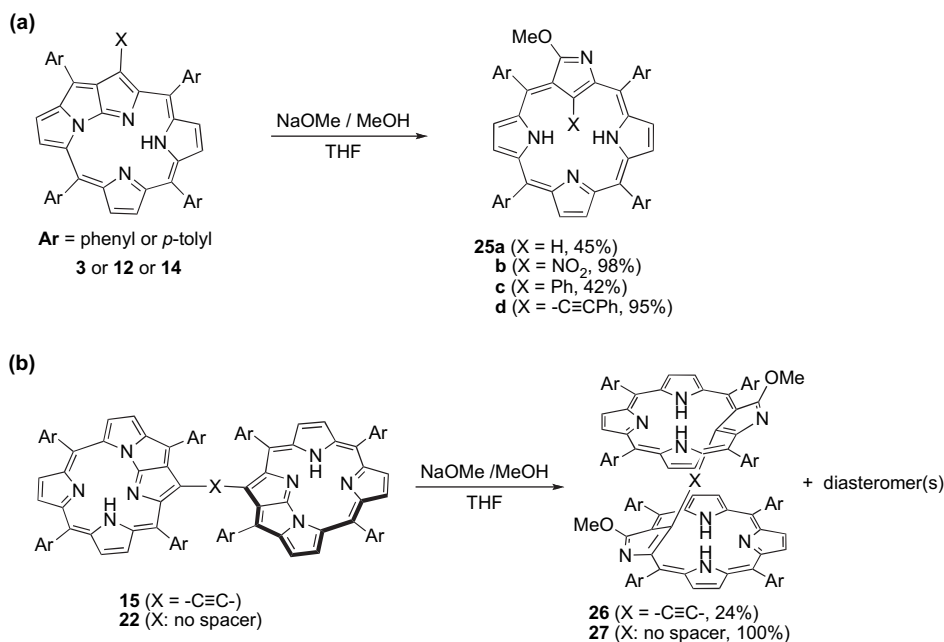
Table 1
Absorption maxima (nm) of NFP derivatives in CH_2Cl_2

Compound	N	S _I	S _{II}	Q _I	Q _{II}	Q _{III}	Q _{IV}
3a ^a	363	499	549	648	702	858	941
12a	348	501	548	647	701	873	967
12b	356	491	549	650	700	903	960
13a	352	432	505	552	650	704	869
13b	352	502	550	648	701	871	954
14	351	424	527	573	666	719	903
15	352	407	516	587	673	733	917
16	358	494	566	652	705	870	988
19	364	417	452	546	593	693	739
20	399	515	567	—	716	862	944
21	370	487	510	556	658	702	—
22 ^b	354	501	571	659	713	887	977
23a ^c	368	501	—	648	—	862	956
23b	371	543	—	676	—	871	—
23c	349	502	533	646	—	867	956
23d	351	503	579	675	—	897	1000
24	351	497	578	634	—	891	1002

^a Ref. 5b.

^b Ref. 5c.

^c Ref. 6a.



Scheme 6.

2.4. Re(I)-coordination of NFP

As mentioned in the introduction section, NFP serves as a monovalent 6-electron donor ligand.^{6a–c} When the 21-substituted NFPs and dimer were subjected to rhenium(I) metal complexation using Re₂(CO)₁₀ in chlorobenzene at 120 °C, rhenium(I) NFP complexes **23a–d** and bismetal complex (**24**) were obtained in 37–88 and 66% yields, respectively (Scheme 5).

2.5. Optical absorption of NFP derivatives

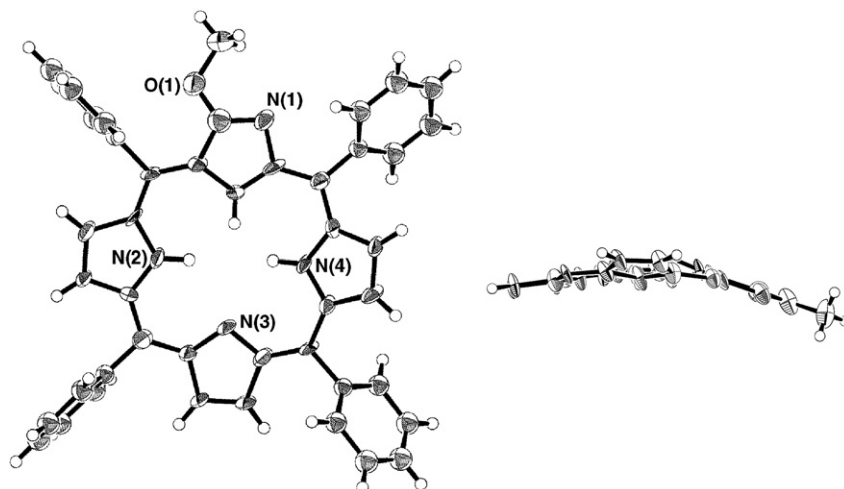
The 21-aryl-substituents affect on the electronic states of NFP only modestly and the optical absorption of **12** was almost same as that of **3b**. On the other hand, the 21-phenylethynyl group causes a strong electronic interaction with NFP core in **14**, showing a large change of the Soret-like band

(400–600 nm) and bathochromic shifts in the absorption spectrum (Fig. 3 and Table 1).

Strong electronic communication is also seen with ethyne-bridged dimer **15**. In the absorption spectrum of **15**, remarkable bathochromic shifts are observed and the absorption maximum of the longest-wavelength band appears at 1020 nm with the tail reaches over 1100 nm, which are shifted by 80 and 100 nm, respectively, compared with those of monomer **3a** (Fig. 3b). Similarly, the optical absorption of Re(I) complex **23** in CH₂Cl₂ shows bathochromic shifts but the number of absorption peaks is not altered, comparing with that of **3a**.^{5b}

2.6. Ring-opening of the fused ring by nucleophiles

One of the characteristic reactions of NFP is a ring-opening reaction, where the strong nucleophiles like alkoxides cleave

Figure 4. X-ray structure of **25a**. Top view (left) and side view (right). *meso*-Phenyl groups are omitted for clarity in the side view.

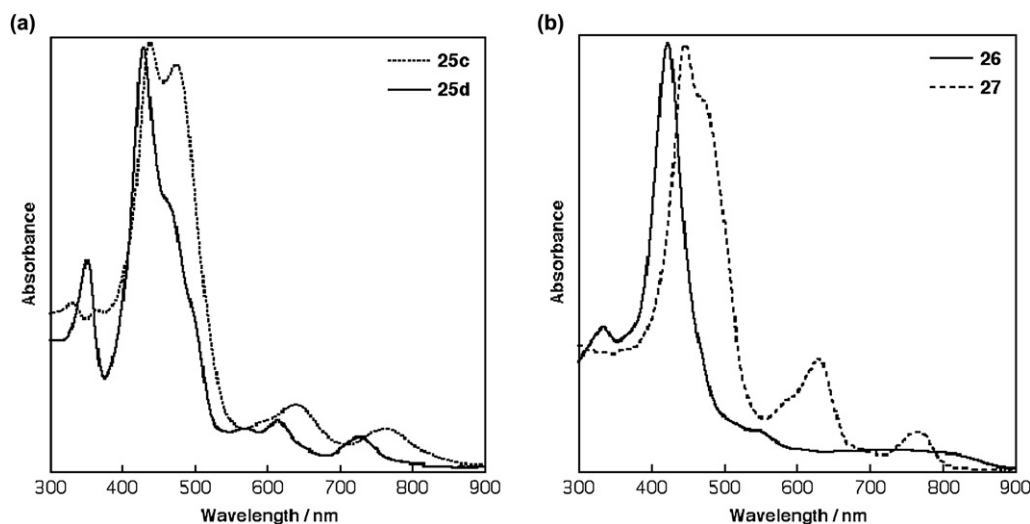


Figure 5. Optical absorption spectra of NFP derivatives **25c**, **25d**, **26**, and **27** in CH_2Cl_2 .

the bridging C–N bond of the fused ring and afford 21-substituted NCPs efficiently (Scheme 6a).⁵ This ring-opening reaction is very useful to obtain various substituted NCPs, especially C21-substituted ones.^{6d} The X-ray structure of ring-opening product, **25a**, for example, is shown in Figure 4. The C3-position of the confused pyrrole is substituted by a methoxy group, which is derived from the methoxide base used in the ring-opening reaction. The porphyrin core of **25a** is relatively planar compared with *N*-confused tetraphenylporphyrin (NCTPP): the mean deviation from the least-square plane is 0.205 Å (vs 0.225 Å for NCTPP), and the confused pyrrole is tilted to the mean plane with the dihedral angle, 20.18° (vs 26.9°).^{3a}

21-Aryl and arylethynyl NFP derivatives were also transformed into 3-methoxy NCP derivatives (**25c** and **25d**) by a treatment with NaOMe/MeOH in THF in 42 and 95% yields, respectively. The 21-substituents of **25c** and **25d** are located on the porphyrin rings. In the ¹H NMR spectra of **25c** and **25d** in CDCl_3 , the proton signals of phenyl group are upfield shifted due to the ring current of the porphyrins and appear at 3.17, 5.29, 5.51 ppm for *o*, *m*, *p*-protons in **25c**, respectively, and at 3.46, 6.07, 6.37 ppm for **25d**, respectively. The ¹H signals of 3-methoxy group are observed at 3.50 ppm for **25c** and 3.78 ppm for **25d**. The optical absorption spectra of both **25c** and **25d** in CH_2Cl_2 showed broad Soret bands due to the distortion by the bulky inner-substituents (Fig. 5a). Particularly, the Soret band of **25c** is split and the absorption maxima are observed at 438 and 473 nm and the number of Q-bands is halved from four peaks of normal porphyrin. On the other hand, the Soret band of **25d** shows a hypsochromic shift with a shoulder at 475 nm.

NFP-dimers **15** and **22** also undergo nucleophilic cleavage and transform into 3,3'-dimethoxy-2,2'-ethyne-bridged NCP dimer (**26**) (24%) and 3,3'-dimethoxy-2,2'-linked NCP dimer (**27**) (>99%),^{5c} respectively (Scheme 6b). The mass peaks of **26** and **27** are in accordance with the supposed structures. The ¹H NMR spectrum of **26** in CDCl_3 is complicated because of the dimer **26** existing as a diastereomeric mixture due to the

face-chirality of NCP. The ¹H NMR spectrum of **27**, on the other hand, exhibits two sets of signals with a signal ratio 100:9, which is also ascribable to the diastereomeric pairs. The observed selectivity of the products might be derived from the steric hindrance of the intermediate, i.e., NCP–NFP hybrid–dimer, during the attack of the second nucleophiles.^{5c} The absorption spectrum of **27** in CH_2Cl_2 displays a broad Soret band with a shoulder at 447 nm and the Q-bands at 629 and 766 nm (Fig. 5b).

3. Summary and conclusions

21-Bromo-substituted NFPs are reactive for palladium-catalyzed cross-coupling reactions under Suzuki and Stille conditions to afford 21-aryl or arylethynyl NFPs. The silver(I) salt promotes the substitution of NFP but, in the absence of nucleophiles, causes a dimerization of NFP linking at C21-positions of the fused rings. Complexation of rhenium(I) metal with NFP and NFP-dimer were also achieved. All the new NFP derivatives display unique absorption spectra, and particularly, ethyne-bridged NFP-dimer exhibits remarkable bathochromic shifts into a near-infrared region, showing an absorption band at 1020 nm with tailing up to 1100 nm. Moreover, the cleavage of C–N bond in the fused ring converts NFP into NCP derivatives. By using this ring-opening reactions, various C3-substituted NCPs including C21,C21'-linked NCP dimers were synthesized from NFP derivatives. As the modification of NCP is facile,¹⁴ such mutual conversion between NCP and NFP may accelerate the development of both *N*-confused and *N*-fused porphyrin chemistry, synergistically.

4. Experimental

4.1. General

Commercially available solvents and reagents were used without further purification unless otherwise mentioned. CDCl_3 (Isotec. Inc.) for NMR measurements was neutralized

with alumina columns. NBS was recrystallized from water. Thin-layer chromatography (TLC) was carried out on aluminum sheets coated with silica gel 60 (Merck 5554). UV/vis spectra were recorded on a Shimadzu UV-3100PC spectrometer. ^1H and ^{13}C NMR spectra were recorded on a JEOL α -500 spectrometer (operating at 500.00 MHz for ^1H and 125.65 MHz for ^{13}C) and a JEOL 300 spectrometer (operating at 300.40 MHz for ^1H) using deuterated solvents as the internal lock and the residual solvents as the internal references. Fast atom bombardment mass spectra (FABMS) and high resolution mass spectra (HRMS) were recorded on a JEOL-HX110 in the positive ion mode with a xenon primary atom beam with 3-nitrobenzyl alcohol matrix. MALDI-TOF mass spectra were recorded on a Voyager-DE RP and Bruker Daltonics autoflex spectrometers in the positive ion mode with dithranol matrix.

4.2. 21-Trifluoromethyl *N*-fused tetraphenylporphyrin (**3e**)

To a CH_2Cl_2 solution of Ni(II) *N*-confused tetraphenylporphyrinate^{3b} (107.1 mg, 0.160 mmol), *S*-(trifluoromethyl)-3,7-dinitro-dibenzothiophenium trifluoromethane-sulfonate (89.75 mg, 0.182 mmol) was added, and the solution was stirred for 30 min under argon. After the solvent was removed under reduced pressure, the residue was purified by column chromatography on silica gel eluted with CH_2Cl_2 . The first green fraction afforded the Ni(II) complex of **2e** (115.7 mg, 0.156 mmol) in 98% yield. ^1H NMR (CDCl_3): δ 10.08 (s, 1H), 8.68 (d, $J=5.0$ Hz, 1H), 8.65 (d, $J=5.0$ Hz, 1H), 8.53 (m, 2H), 8.49 (d, $J=5.0$ Hz, 1H), 8.45 (d, $J=4.5$ Hz, 1H), 8.13 (m, 4H), 7.76 (m, 16H). UV/vis (CH_2Cl_2): λ_{max} [nm]=720, 592, 434, 325. FABMS: $m/z=739.2$ (calcd for $\text{C}_{45}\text{H}_{28}\text{N}_4\text{F}_3\text{Ni} [\text{M}+\text{H}^+]$ 739.1620).

The Ni(II) complex was dissolved in a mixed solvent of CH_2Cl_2 (10 mL) and TFA (10 mL), and the solution was stirred for 48 h. The reaction mixture was neutralized, washed with aqueous NaHCO_3 , and dried over Na_2SO_4 . After evaporation, the residues were purified by column chromatography on silica gel eluted with 3% MeOH– CH_2Cl_2 . After evaporation, the residue was recrystallized to afford **2e** (65.5 mg, 0.096 mmol) in 62% yield. ^1H NMR (CDCl_3): δ 9.09 (m, 2H), 8.67 (m, 2H), 8.46 (m, 6H), 8.14 (m, 4H), 7.89 (m, 5H), 7.76 (m, 7H), 7.03 (s, 1H), two inner NH signals were not observed at 25 °C. UV/vis (CH_2Cl_2): λ_{max} [nm]=734, 609, 564, 457. FABMS: $m/z=682.4$ (calcd for $\text{C}_{45}\text{H}_{29}\text{N}_4\text{F}_3 [\text{M}^+]$ 682.2344).

To a solution of **2e** (19.53 mg, 0.0286 mmol) in CH_2Cl_2 (20 mL), NBS (5.33 mg, 0.0299 mmol) was added and stirred for 10 min. Then, the reaction mixture was washed with water and dried over Na_2SO_4 and the solvent was evaporated under reduced pressure. Without isolation of **8e**, the residue was dissolved into pyridine (20 mL) and stirred for 3 h at 80 °C. The solvent was removed under reduced pressure and the residue was purified by column chromatography on silica gel eluted with 1% MeOH– CH_2Cl_2 . The first red fraction contained **11e**, the second one **9e**, and the third one **3e**. Each fraction was evaporated and the residues were recrystallized from CH_2Cl_2 –MeOH to afford green crystals of **11e**, **9e**, and **3e**,

in trace amount, 5.2 mg (24% in two steps), and 6.9 mg (35%), respectively. Compound **3e**: ^1H NMR (CDCl_3): δ 9.05 (d, $J=5.0$ Hz, 1H), 8.86 (d, $J=4.5$ Hz, 1H), 8.35 (d, $J=7.5$ Hz, 2H), 8.25 (d, $J=4.0$ Hz, 1H), 8.23 (d, $J=4.5$ Hz, 1H), 8.18 (m, 3H), 8.10 (dd, $J=8.0$, 1.5 Hz, 2H), 8.05 (dd, $J=8.0$, 1.5 Hz, 2H), 7.82 (d, $J=4.5$ Hz, 1H), 7.73 (m, 11H), 7.62 (t, $J=7.5$ Hz, 1H), 6.63 (br s, 1H). UV/vis (CH_2Cl_2): λ_{max} [nm]=881, 805, 692, 637, 531(sh), 498, 364. FABMS: $m/z=680.287$ (calcd for $\text{C}_{45}\text{H}_{27}\text{N}_4\text{F}_3 [\text{M}^+]$ 680.2188). Compound **9e**: ^1H NMR (CDCl_3): δ 8.95 (d, $J=5.0$ Hz, 1H), 8.73 (d, $J=4.5$ Hz, 1H), 8.29 (m, 4H), 8.09 (m, 5H), 7.79 (m, 4H), 7.83 (d, $J=4.5$ Hz, 1H), 7.73 (m, 8H), 7.60 (t, $J=7.0$ Hz, 1H), 6.12 (br s, 1H). UV/vis (CH_2Cl_2): λ_{max} [nm]=860, 822, 633, 497, 368. FABMS: $m/z=758.317$ (calcd for $\text{C}_{45}\text{H}_{26}\text{N}_4\text{F}_3\text{Br} [\text{M}^+]$ 758.1293).

4.3. 21-Phenyl *N*-fused tetrakis(*p*-tolyl)porphyrin (**12a**)

A mixture of **3b** (30.10 mg, 0.0463 mmol), $\text{PhB}(\text{OH})_2$ (49.42 mg, 0.408 mmol), K_2CO_3 (164.83 mg, 1.19 mmol), and $\text{Pd}(\text{PPh}_3)_4$ (5.2 mg, 0.0045 mmol) was dissolved in distilled toluene (3 mL), and degassed by repeated freeze–pump–thaw cycles. The solution was stirred for 3 h under Ar at 90 °C. After washing with water and drying over anhydrous Na_2SO_4 , the solvent was removed under reduced pressure. The residue was purified by column chromatography on silica gel eluted with 5% MeOH– CH_2Cl_2 . The bright reddish fraction was collected and the solvent was evaporated to dryness. The residue was recrystallized from CH_2Cl_2 –MeOH to afford luster green crystals of **12a** (21.0 mg) in 70% yield. ^1H NMR (CDCl_3): δ 8.92 (d, $J=5.2$ Hz, 1H), 8.61 (br s, 1H), 8.57 (d, $J=5.2$ Hz, 1H), 8.05 (d, $J=4.8$ Hz, 1H), 7.95 (m, 4H), 7.87 (d, $J=8.0$ Hz, 2H), 7.77 (d, $J=8.0$ Hz, 2H), 7.62 (d, $J=8.0$ Hz, 2H), 7.59 (d, $J=4.4$ Hz, 1H), 7.49 (d, $J=8.0$ Hz, 2H), 7.47 (d, $J=8.0$ Hz, 2H), 7.31 (d, $J=8.0$ Hz, 2H), 7.19 (m, 3H), 7.08 (t, $J=7.6$ Hz, 2H), 7.02 (d, $J=8.0$ Hz, 2H), 2.67 (s, 3H), 2.60 (s, 3H), 2.44 (s, 3H), 2.41 (s, 3H). ^{13}C NMR (CDCl_3): δ 157.11, 153.50, 150.60, 147.94, 146.85, 143.74, 142.25, 139.29, 137.95, 137.66, 137.23, 137.17, 137.11, 136.54, 136.47, 135.09, 134.28, 134.19, 132.94, 132.93, 132.76, 132.05, 131.76, 131.42, 157.11, 153.50, 150.60, 147.94, 146.85, 143.74, 142.25, 139.29, 137.95, 137.66, 137.24, 137.17, 137.11, 136.54, 136.47, 135.09, 134.28, 134.19, 132.94, 132.93, 132.76, 132.05, 131.76, 131.42, 129.81, 129.33, 128.69, 128.48, 127.84, 127.61, 126.67, 126.38, 125.26, 124.84, 124.20, 119.49, 118.32, 115.10, 21.54, 21.41, 21.35, 21.25. UV/vis (CH_2Cl_2): λ_{max} [nm] (log ϵ)=967 (3.52), 873 (3.50), 701 (3.75), 647 (3.94), 548 (4.67), 501 (4.69), 348 (4.57). HRMS: calcd for $\text{C}_{54}\text{H}_{41}\text{N}_4 [\text{M}+\text{H}^+]$, 745.3331; found 745.3385.

4.4. 21-(2'-Methoxyphenyl) *N*-fused tetrakis(*p*-tolyl)porphyrin (**12b**)

A mixture of **3b** (10.28 mg, 0.0137 mmol), 2-methoxyphenylboronic acid (21.40 mg, 0.141 mmol), K_2CO_3 (20.25 mg, 0.146 mmol), and $\text{Pd}(\text{PPh}_3)_4$ (4.14 mg, 0.0036 mmol) was

dissolved in distilled toluene (2 mL), and degassed by repeated freeze–pump–thaw cycles. The solution was stirred for 5 h under Ar at 90 °C. After washing with water and drying over anhydrous Na₂SO₄, the solvent was removed under reduced pressure. The residue was purified by column chromatography on silica gel eluted with 3% MeOH–CH₂Cl₂. The bright reddish fraction was collected and the solvent was evaporated to dryness. The residue was recrystallized from CH₂Cl₂–hexane to afford luster green crystals of **12b** (6.11 mg) in 58% yield. ¹H NMR (CDCl₃): δ 9.02 (d, *J*=5.4 Hz, 1H), 8.64 (d, *J*=5.1 Hz, 1H), 8.04 (d, *J*=7.8 Hz, 2H), 7.94 (d, *J*=6.9 Hz, 2H), 7.82 (d, *J*=8.1 Hz, 4H), 7.76 (m, 2H), 7.69 (d, *J*=4.2 Hz, 1H), 7.52 (m, 8H), 7.23 (m, 4H), 6.70 (m, 2H), 3.25 (s, 3H), 2.68 (s, 3H), 2.62 (s, 3H), 2.46 (s, 3H), 2.39 (s, 3H). UV/vis (CH₂Cl₂): λ_{max} [nm]=960 (3.51), 903 (3.56), 700 (3.61), 650 (3.85), 549 (4.46), 491 (4.56), 356 (4.47). HRMS: calcd for C₅₅H₄₃N₄O [M+H⁺], 775.3437; found 775.3328.

4.5. *N*-Fused porphyrin (**3a**) via palladium-catalyzed debromination

A mixture of **3b** (13.05 mg, 0.0175 mmol), pentafluorophenylboronic acid (38.99 mg, 0.184 mmol), K₂CO₃ (26.40 mg, 0.190 mmol), and Pd(PPh₃)₄ (3.92 mg, 0.0034 mmol) was dissolved in distilled toluene (2 mL), and degassed by repeated freeze–pump–thaw cycles. The solution was stirred for 15 h under Ar at 90 °C. After washing with water and drying over anhydrous Na₂SO₄, the solvent was removed under reduced pressure. The residue was purified by column chromatography on silica gel eluted with 5% MeOH–CH₂Cl₂. The bright reddish fraction was collected and the solvent was evaporated to dryness. The residue was recrystallized from CH₂Cl₂–hexane to afford luster green crystals of **3a** (11.45 mg) in 98% yield.

4.6. 21-(2'-Furyl) *N*-fused tetrakis(*p*-tolyl)porphyrin (**13a**)

A mixture of **3b** (10.83 mg, 0.0145 mmol) and Pd(PPh₃)₄ (2.72 mg, 0.00235 mmol) was dissolved in distilled toluene (2 mL), and degassed by repeated freeze–pump–thaw cycles. 2-(Tributylstannyl)furan (45 μL, 0.143 mmol) was added to the reaction mixture under Ar and stirred for 15 h at 100 °C. After washing with water and drying over anhydrous Na₂SO₄, the solvent was removed under reduced pressure. The residue was purified by column chromatography on silica gel eluted with 5% MeOH–CH₂Cl₂. The red fraction was collected and the solvent was evaporated to dryness. The residue was recrystallized from CH₂Cl₂–hexane to afford violet crystals of **13a** (8.2 mg) in 77% yield. ¹H NMR (CDCl₃): δ 9.03 (d, *J*=4.8 Hz, 1H), 8.69 (d, *J*=5.4 Hz, 2H), 8.21 (d, *J*=5.1 Hz, 1H), 8.02–7.85 (m, 8H), 7.75 (d, *J*=4.2 Hz, 2H), 7.53 (d, *J*=7.8 Hz, 2H), 7.49 (d, *J*=7.8 Hz, 2H), 7.37 (d, *J*=8.1 Hz, 2H), 7.34 (m, 3H), 7.30 (m, 1H), 6.33 (dd, *J*=3.0, 1.5 Hz, 1H), 6.09 (d, *J*=2.7 Hz, 1H), 2.68 (s, 3H), 2.62 (s, 3H), 2.53 (s, 3H), 2.51 (s, 3H). UV/vis (CH₂Cl₂): λ_{max} [nm] (log ε)=940 (3.46), 869 (3.44), 704 (3.77), 650 (3.94), 552

(4.61), 505 (4.62), 432 (4.51), 352 (4.58). HRMS: calcd for C₅₂H₃₉N₄O [M+H⁺], 735.3124; found 735.3267.

4.7. 2-(2'-Thienyl)-*N*-fused tetrakis-*p*-tolylporphyrin (**13b**)

A mixture of **3b** (11.48 mg, 0.0154 mmol) and Pd(PPh₃)₄ (2.53 mg, 0.00219 mmol) was dissolved in distilled toluene (2 mL), and degassed by repeated freeze–pump–thaw cycles. 2-(Tributylstannyl)thiophene (50 μL, 0.0157 mmol) was added to the reaction mixture under Ar and stirred for 15 h at 100 °C. After washing with water and drying over anhydrous Na₂SO₄, the solvent was removed under reduced pressure. The residue was purified by column chromatography on silica gel eluted with 5% MeOH–CH₂Cl₂. The red fraction was collected and the solvent was evaporated to dryness. The residue was recrystallized from CH₂Cl₂–hexane. A violet crystal of **13b** (9.35 mg) was obtained in 81% yield. ¹H NMR (CDCl₃): δ 8.97 (d, *J*=5.1 Hz, 1H), 8.63 (d, *J*=5.4 Hz, 1H), 8.10 (d, *J*=4.8 Hz, 1H), 7.96 (m, 5H), 7.88 (dd, *J*=8.1, 1.8 Hz, 4H), 7.77 (d, *J*=7.5 Hz, 2H), 7.66 (d, *J*=4.5 Hz, 1H), 7.49 (m, 5H), 7.30 (m, 1H), 7.16 (d, *J*=7.8 Hz, 2H), 6.86–6.81 (m, 2H), 2.67 (s, 3H), 2.60 (s, 3H), 2.48 (s, 3H), 2.46 (s, 3H), the inner NH signal was not observed. UV/vis (CH₂Cl₂): λ_{max} [nm] (log ε)=954 (3.51), 871 (3.50), 701 (3.73), 648 (3.94), 550 (4.64), 502 (4.64), 352 (3.50). HRMS: calcd for C₅₂H₃₉N₄S [M⁺+H], 751.2895; found 751.2997.

4.8. 21-Phenylethynyl *N*-fused tetrakis(*p*-tolyl)porphyrin (**14**)

A mixture of **3b** (20.03 mg, 0.0268 mmol) and Pd(PPh₃)₄ (4.81 mg, 0.0042 mmol) was dissolved in distilled toluene (2 mL), and degassed by repeated freeze–pump–thaw cycles. Phenylethynyl-tributyltin (93 mL, 0.265 mmol) was added to the reaction mixture under Ar and the solution was stirred for 2 h at 100 °C. After washing with water and drying over anhydrous Na₂SO₄, the solvent was removed under reduced pressure. The residue was purified by column chromatography on silica gel eluted with 5% MeOH–CH₂Cl₂. The purple fraction was collected and the solvent was evaporated to dryness. The residue was recrystallized from CH₂Cl₂–MeOH to afford violet crystals of **14** (16.3 mg) in 79% yield. ¹H NMR (CDCl₃): δ 9.01 (d, *J*=5.4 Hz, 1H), 8.77 (d, *J*=8.4 Hz, 2H), 8.61 (d, *J*=5.1 Hz, 1H), 8.21 (br s, 1H), 8.13 (d, *J*=7.8 Hz, 2H), 8.05 (d, *J*=4.5 Hz, 1H), 8.00 (m, 2H), 7.94 (d, *J*=7.8 Hz, 2H), 7.86 (d, *J*=7.8 Hz, 2H), 7.65 (m, 4H), 7.53 (m, 7H), 7.34 (m, 2H), 7.25 (m, 1H), 2.67 (s, 3H), 2.63 (s, 3H), 2.60 (s, 3H), 2.57 (s, 3H). ¹³C NMR (CDCl₃): δ 157.15, 154.26, 151.12, 150.63, 146.28, 143.44, 142.07, 139.66, 138.79, 138.13, 138.02, 137.32, 136.73, 136.25, 134.79, 134.64, 134.21, 133.98, 133.51, 132.96, 131.94, 131.58, 131.07, 130.44, 130.05, 129.89, 128.56, 128.49, 128.04, 127.61, 127.42, 125.43, 124.79, 124.53, 119.75, 116.28, 103.88, 102.63, 88.51, 21.52, 21.40. UV/vis (CH₂Cl₂): λ_{max} [nm] (log ε)=999 (3.56), 903 (3.60), 719 (4.20), 666 (4.23), 573 (4.88), 527 (4.69), 424 (4.67), 351 (4.73). HRMS: calcd for C₅₆H₄₁N₄ [M+H⁺], 769.3331; found 769.3267.

4.9. Bis[2-*N*-fused tetrakis(*p*-tolyl)porphyrinyl]-acetylene (**15**)

A mixture of **3b** (21.49 mg, 0.0288 mmol) and Pd(PPh₃)₄ (2.76 mg, 0.0024 mmol) was dissolved in distilled toluene (2 mL), and degassed by repeated freeze–pump–thaw cycles. After filling Ar gas in the reaction tube, bis(tributylstannyl)-acetylene (7.5 mL, 0.014 mmol) was added to the reaction mixture and stirred for 5 h at 100 °C. After washing with water and drying over anhydrous Na₂SO₄, the solvent was removed under reduced pressure. The residue was purified by flash-column chromatography on silica gel eluted with 2% MeOH–CH₂Cl₂. The second purple fraction was collected and the solvent was evaporated to dryness. The residue was recrystallized from CH₂Cl₂–MeOH to afford violet crystals of **15** (9.8 mg) in 50% yield. ¹H NMR (CDCl₃): δ 9.05 (d, *J*=5.1 Hz, 2H), 8.80 (br s, 2H), 8.72 (d, *J*=8.4 Hz, 2H), 8.40 (d, *J*=5.1 Hz, 2H), 8.21 (d, *J*=8.4 Hz, 4H), 8.61 (d, *J*=5.1 Hz, 2H), 8.04 (d, *J*=4.5 Hz, 2H), 7.93 (m, 12H), 7.61 (d, *J*=4.5 Hz, 2H), 7.50 (d, *J*=7.5 Hz, 8H), 7.11 (d, *J*=7.8 Hz, 4H), 6.64 (br s, 4H), 2.70 (s, 6H), 2.60 (s, 6H), 2.09 (s, 6H), 0.89 (s, 6H). UV/vis (CH₂Cl₂): λ_{max} [nm] (log ε)=1020 (3.67), 917 (3.80), 733 (4.40), 673 (4.39), 587 (4.78), 516 (4.70), 407 (4.78), 352 (4.76). MALDI-TOFMS: *m/z*=1359.52 (calcd for C₉₈H₇₁N₈ [M+H⁺], 1359.58).

4.10. 17,18,21-Triphenyl *N*-fused tetrakis(*p*-tolyl)-porphyrin (**16**)

A mixture of **11b** (20.91 mg, 0.0231 mmol), phenylboronic acid (85.38 mg, 0.704 mmol), K₂CO₃ (99.73 mg, 0.719 mmol), and Pd(PPh₃)₄ (8.16 mg, 0.00706 mmol) was dissolved in distilled toluene (5 mL), and degassed by repeated freeze–pump–thaw cycles. The solution was stirred for 3 h under Ar at 100 °C. After washing with water and drying over anhydrous Na₂SO₄, the solvent was removed under reduced pressure. The residue was purified by column chromatography on silica gel eluted with 5% MeOH–CH₂Cl₂. The bright red fraction was collected and the solvent was evaporated to dryness. The residue was recrystallized from CH₂Cl₂–MeOH to afford luster green crystals of **16** (8.4 mg) in 41% yield. Due to the low solubility in CDCl₃, the ¹H NMR spectral data were unable to obtain. UV/vis (CH₂Cl₂): λ_{max} [nm]=988 (3.73), 870 (3.81), 705 (3.95), 652 (4.08), 566 (4.66), 494 (4.78), 358 (4.69). HRMS: calcd for C₆₆H₄₉N₄ [M+H⁺], 897.3957; found 897.3894.

4.11. 17,18-Dibromo-*N*-fused porphyrin (**11a**) from **11b**

A mixture of **11b** (24.64 mg, 0.0272 mmol), 2,4-dimethoxyphenylboronic acid (99.68 mg, 0.548 mmol), K₂CO₃ (76.70 mg, 0.553 mmol), and Pd(PPh₃)₄ (5.48 mg, 0.00474 mmol) was dissolved in distilled toluene (2 mL), and degassed by repeated freeze–pump–thaw cycles. The solution was stirred for 15 h under Ar at 100 °C. After washing with water and drying over anhydrous Na₂SO₄, the solvent was removed under reduced pressure. The residue was purified by

column chromatography on silica gel eluted with CH₂Cl₂. The second red fraction was collected and the solvent was evaporated to dryness. The residue was recrystallized from CH₂Cl₂–hexane to afford green crystals of **11a** (17.9 mg) in 80% yield.

4.12. 17,18-Diphenyl *N*-confused tetrakis(*p*-tolyl)-porphyrin (**18**)

A mixture of **11b** (20.00 mg, 0.0242 mmol), phenylboronic acid (31.43 mg, 0.259 mmol), K₂CO₃ (36.46 mg, 0.263 mmol), and Pd(PPh₃)₄ (2.93 mg, 0.0025 mmol) was dissolved in distilled toluene (3 mL), and degassed by repeated freeze–pump–thaw cycles. The solution was stirred for 3 h under Ar at 100 °C. After washing with water and drying over anhydrous Na₂SO₄, the solvent was removed under reduced pressure. The residue was purified by column chromatography on silica gel eluted with 2% MeOH–CH₂Cl₂. The bright green fraction was collected and the solvent was evaporated to dryness. The residue was recrystallized from CH₂Cl₂–MeOH to afford luster green crystals of **18** (13.8 mg) in 69% yield. ¹H NMR (CDCl₃): δ 8.62 (d, *J*=5.7 Hz, 1H), 8.33 (d, *J*=5.1 Hz, 1H), 8.17 (s, 2H), 8.10 (d, *J*=8.1 Hz, 2H), 7.95 (m, 4H), 7.58 (d, *J*=7.5 Hz, 2H), 7.51 (m, 4H), 7.27 (m, 1H), 7.17 (t, *J*=8.1 Hz, 2H), 7.06 (d, *J*=7.8 Hz, 2H), 6.96 (m, 4H), 6.86 (m, 6H), 2.64 (s, 3H), 2.62 (s, 3H), 2.44 (s, 3H), 2.32 (s, 3H), –1.13 (s, 1H at –40 °C), –1.45 (s, 1H at –40 °C), –3.34 (s, 1H). ¹³C NMR (CDCl₃): δ 165.10, 159.54, 155.32, 155.09, 145.83, 141.56, 139.07, 138.67, 138.37, 137.95, 137.36, 137.25, 137.22, 137.19, 137.15, 136.76, 135.62, 135.37, 135.33, 134.91, 134.65, 134.62, 134.53, 134.48, 133.72, 132.14, 132.04, 131.92, 128.67, 128.54, 128.39, 127.87, 127.65, 127.25, 126.91, 126.70, 126.60, 126.30, 125.59, 125.35, 124.44, 123.24, 123.13, 119.53, 119.02, 114.92, 102.15, 21.44, 21.40, 21.26, 21.18. UV/vis (CH₂Cl₂): λ_{max} [nm]=723 (3.85), 612 (4.21), 563 (4.06), 454 (5.08). HRMS: calcd for C₆₀H₄₇N₄ [M+H⁺], 823.3801; found 823.3778.

4.13. 17,18,21-Tris(phenylethynyl) *N*-fused tetrakis(*p*-tolyl)porphyrin (**19**)

A mixture of **11b** (22.19 mg, 0.0245 mmol) and Pd(PPh₃)₄ (5.14 mg, 0.0044 mmol) was dissolved in distilled toluene (2 mL), and degassed by repeated freeze–pump–thaw cycles. Phenylethynyl-tributyltin (127 mL, 0.291 mmol) was added to the reaction mixture under Ar and stirred for 12 h at 90 °C. After washing with water and drying over anhydrous Na₂SO₄, the solvent was removed under reduced pressure. The residue was purified by column chromatography on silica gel eluted with 1% MeOH–CH₂Cl₂. The purple fraction was collected and the solvent was evaporated to dryness. The residue was recrystallized from CH₂Cl₂–MeOH to afford violet crystals of **19** (11.79 mg) in 50% yield. ¹H NMR (CDCl₃): δ 8.87 (d, *J*=4.8 Hz, 1H), 8.69 (d, *J*=8.4 Hz, 2H), 8.40 (d, *J*=5.1 Hz, 1H), 8.21 (d, *J*=7.5 Hz, 2H), 8.06 (d, *J*=4.8 Hz, 1H), 7.97 (d, *J*=7.8 Hz, 2H), 7.79 (d, *J*=7.5 Hz, 2H), 7.60 (d, *J*=4.2 Hz, 1H), 7.53 (m, 4H), 7.47 (d, *J*=8.1 Hz, 4H), 7.33 (m, 4H),

7.26 (m, 9H), 7.18 (m, 2H), 6.96 (br s, 1H), 2.66 (s, 3H), 2.56 (s, 3H), 2.54 (s, 3H), 2.51 (s, 3H). UV/vis (CH₂Cl₂): λ_{\max} [nm]=997 (3.60), 908 (3.66), 739 (4.29), 693 (4.17), 593 (4.59), 546 (4.64), 452 (4.70), 417 (4.69), 364 (4.61). HRMS: calcd for C₇₂H₄₉N₄ [M+H⁺], 969.3957; found 969.4008.

4.14. 17,18-Bis(phenylethynyl) N-fused tetrakis(p-tolyl)porphyrin (**20**)

A mixture of **11a** (12.93 mg, 0.0156 mmol) and Pd(PPh₃)₄ (3.01 mg, 0.0026 mmol) was dissolved in distilled toluene (2 mL), and degassed by repeated freeze–pump–thaw cycles. Phenylethynyl-tributyltin (100 μ L, 0.229 mmol) was added to the reaction mixture under Ar and stirred for 5 h at 100 °C. After washing with water and drying over anhydrous Na₂SO₄, the solvent was removed under reduced pressure. The residue was purified by column chromatography on silica gel eluted with 2% MeOH–CH₂Cl₂. The purple fraction was collected and the solvent was evaporated to dryness. The residue was recrystallized from CH₂Cl₂–MeOH to afford violet crystals of **20** (12.3 mg) in 91% yield. ¹H NMR (CDCl₃): δ 9.22 (s, 1H), 8.92 (d, *J*=5.1 Hz, 1H), 8.57 (d, *J*=7.5 Hz, 2H), 8.35 (m, 3H), 8.07 (d, *J*=4.8 Hz, 1H), 8.00 (d, *J*=7.8 Hz, 2H), 7.78 (d, *J*=7.5 Hz, 2H), 7.71 (br s, 1H), 7.64 (d, *J*=7.8 Hz, 2H), 7.55 (m, 7H), 7.18 (m, 10H), 2.66 (s, 3H), 2.64 (s, 3H), 2.54 (s, 6H). UV/vis (CH₂Cl₂): λ_{\max} [nm] (log ϵ)=944 (3.63), 862 (3.59), 716 (3.85), 567 (4.28), 515 (4.69), 399 (4.60). HRMS: calcd for C₆₄H₄₅N₄ [M+H⁺], 869.3644; found 869.3615.

4.15. 2-(N'-Pyridyl)-N-fused tetraphenylporphyrin (**21**)

To a solution of **3a** (Ar=phenyl) (12.01 mg, 0.0174 mmol) in pyridine (20 mL), silver trifluoroacetate (38.56 mg, 0.175 mmol) was added and the solution was refluxed for 20 h. The solvent was removed under reduced pressure and the residue was purified by column chromatography on silica gel eluted with 10% MeOH–CH₂Cl₂. A polar red fraction was collected and the solvent was evaporated to dryness. The residue was recrystallized from CH₂Cl₂–hexane to afford violet crystals of **21**·(OCOCF₃)[−] (7.3 mg) in 50% yield. ¹H NMR (CDCl₃): δ 9.23 (d, *J*=5.0 Hz, 1H), 8.99 (d, *J*=5.0 Hz, 1H), 8.55 (d, *J*=5.0 Hz, 1H), 8.70 (m, 2H), 8.32 (m, 3H), 8.08 (m, 6H), 7.92 (d, *J*=5.0 Hz, 1H), 7.78 (m, 10H), 7.56 (m, 4H), 7.58 (m, 2H), 6.12 (s, 1H). UV/vis (CH₂Cl₂): λ_{\max} [nm]=702, 658, 556, 510, 487, 370. FABMS: *m/z*=690.25 (calcd for C₄₉H₃₂N₅ [M–OCOCF₃][−]) 690.2658).

4.16. Rhenium(I) N-fused tetrakis(p-tolyl)porphyrinate (**23a**)

To a solution of **3a** (6.53 mg, 0.00976 mmol) in chlorobenzene (10 mL), Re₂(CO)₁₀ (15.30 mg, 0.023 mmol) was added and stirred at 120 °C for 16 h. The solvent was evaporated under reduced pressure and the residue was purified by column chromatography on silica gel eluted with CH₂Cl₂. The first purple fraction was collected and the solvent was evaporated to dryness. The residue was recrystallized from CH₂Cl₂–hexane to afford violet crystals of **23a** (6.62 mg) in 72% yield.

¹H NMR (CDCl₃): δ 9.29 (s, 1H), 9.17 (d, *J*=5.1 Hz, 1H), 8.75 (d, *J*=4.8 Hz, 1H), 8.59 (d, *J*=8.1 Hz, 2H), 8.10 (d, *J*=8.1 Hz, 2H), 7.90 (d, *J*=7.5 Hz, 2H), 7.75 (m, 3H), 7.62 (d, *J*=7.8 Hz, 2H), 7.56 (d, *J*=7.8 Hz, 2H), 7.51 (d, *J*=7.8 Hz, 2H), 7.47 (d, *J*=4.2 Hz, 1H), 7.40 (d, *J*=7.5 Hz, 2H), 7.35 (d, *J*=5.1 Hz, 1H), 7.23 (d, *J*=4.5 Hz, 1H), 2.68 (s, 3H), 2.67 (s, 3H), 2.56 (s, 6H). UV/vis (CH₂Cl₂): λ_{\max} [nm]=956, 862, 648, 501, 368. MALDI-TOFMS: *m/z*=852.3 (calcd for C₄₈H₃₅N₄Re [M⁺–3CO] 854.24).

4.17. Rhenium(I) 21-nitro N-fused tetrakis(p-tolyl)porphyrinate (**23b**)

To a solution of **3c** (5.97 mg, 0.00836 mmol) in chlorobenzene (10 mL), Re₂(CO)₁₀ (5.94 mg, 0.0090 mmol) was added and stirred at 120 °C for 24 h. The solvent was evaporated under reduced pressure and the residue was purified by column chromatography on silica gel eluted with CH₂Cl₂. The first purple fraction was collected and the solvent was evaporated to dryness. The residue was recrystallized from CH₂Cl₂–hexane to afford violet crystals of **23b** (7.21 mg) in 88% yield. ¹H NMR (CDCl₃): δ 9.15 (d, *J*=4.8 Hz, 1H), 8.98 (d, *J*=5.4 Hz, 1H), 8.09 (d, *J*=8.1 Hz, 2H), 8.04 (d, *J*=4.8 Hz, 1H), 7.95 (d, *J*=8.1 Hz, 2H), 7.77 (d, *J*=7.8 Hz, 2H), 7.65 (d, *J*=4.8 Hz, 1H), 7.56 (m, 4H), 7.47 (m, 4H), 7.40 (d, *J*=4.8 Hz, 1H), 7.24 (d, *J*=4.8 Hz, 1H), 7.18 (d, *J*=7.2 Hz, 2H), 2.69 (s, 3H), 2.61 (s, 3H), 2.59 (s, 3H), 2.57 (s, 3H). UV/vis (CH₂Cl₂): λ_{\max} [nm] (log ϵ)=871 (3.27), 676 (3.63), 543 (4.54), 371 (4.33). MALDI-TOFMS: *m/z*=927.0 (calcd for C₄₉H₃₄N₅O₃Re [M⁺–2CO] 927.22).

4.18. Rhenium(I) 21-phenyl N-fused tetrakis(p-tolyl)porphyrinate (**23c**)

To a solution of **12a** (6.08 mg, 0.00816 mmol) in chlorobenzene (10 mL), Re₂(CO)₁₀ (6.32 mg, 0.0097 mmol) was added and stirred at 120 °C for 15 h. The solvent was evaporated under reduced pressure and the residue was purified by column chromatography on silica gel eluted with CH₂Cl₂. The first purple fraction was collected and the solvent was evaporated to dryness. The residue was recrystallized from CH₂Cl₂–hexane to afford violet crystals of **23c** (6.33 mg) in 76% yield. ¹H NMR (CDCl₃): δ 8.97 (d, *J*=5.7 Hz, 1H), 8.71 (d, *J*=5.7 Hz, 1H), 7.91 (d, *J*=8.1 Hz, 2H), 7.78 (d, *J*=5.1 Hz, 1H), 7.71 (m, 5H), 7.51 (d, *J*=7.5 Hz, 2H), 7.40 (d, *J*=8.4 Hz, 2H), 7.32 (m, 4H), 7.23 (m, 5H), 7.10 (m, 4H), 2.66 (s, 3H), 2.55 (s, 3H), 2.45 (s, 3H), 2.38 (s, 3H). UV/vis (CH₂Cl₂): λ_{\max} [nm] (log ϵ)=956 (3.29), 867 (3.30), 646 (3.63), 533 (4.52), 502 (4.49), 349 (4.41). MALDI-TOFMS: *m/z*=1016.1 (calcd for C₅₇H₃₉N₄O₃Re [M⁺] 1014.26).

4.19. Rhenium(I) 21-phenylethynyl N-fused tetrakis(p-tolyl)porphyrinate (**23d**)

To a solution of **14** (5.16 mg, 6.71 μ mol) in chlorobenzene (10 mL), Re₂(CO)₁₀ (4.85 mg, 0.0074 mmol) was added and

stirred at 120 °C for 12 h. The solvent was evaporated under reduced pressure and the residue was purified by column chromatography on silica gel eluted with CH₂Cl₂. The first purple fraction was collected and the solvent was evaporated to dryness. The residue was recrystallized from CH₂Cl₂–hexane to afford violet crystals of **23d** (2.56 mg) in 37% yield. ¹H NMR (CDCl₃): δ 9.05 (d, *J*=4.8 Hz, 1H), 8.70 (d, *J*=5.4 Hz, 1H), 8.64 (d, *J*=8.1 Hz, 2H), 7.93 (br, 2H), 7.89 (d, *J*=8.4 Hz, 2H), 7.73 (m, 3H), 7.52 (m, 8H), 7.38 (m, 7H), 7.23 (s, 1H, overlapped with solvent), 2.66 (s, 3H), 2.56 (s, 9H). UV/vis (CH₂Cl₂): λ_{max} [nm] (log ε)=1000 (3.45), 897 (3.45), 675 (4.03), 579 (4.73), 503 (4.59), 351 (4.64). MALDI-TOFMS: *m/z*=1040.2 (calcd for C₅₉H₃₉N₄O₃Re [M⁺] 1038.26).

4.20. Bis[rhenium(I) *N*-fused tetrakis(*p*-tolyl)porphyrinate] (**24**)

To a solution of **22** (4.93 mg, 0.00369 mmol) in chlorobenzene (10 mL), Re₂(CO)₁₀ (5.30 mg, 0.0081 mmol) was added and stirred at 120 °C for 18 h. The solvent was evaporated under reduced pressure and the residue was purified by column chromatography on silica gel eluted with CH₂Cl₂. The first purple fraction was collected and the solvent was evaporated to dryness. The residue was recrystallized from CH₂Cl₂–hexane to afford violet crystals of **24** (4.53 mg) in 66% yield. Spectral data for the major diastereomer: ¹H NMR (CDCl₃): δ 9.21 (d, *J*=5.1 Hz, 2H), 8.92 (d, *J*=4.8 Hz, 2H), 8.31 (d, *J*=7.8 Hz, 4H), 8.03 (d, *J*=7.8 Hz, 4H), 7.81 (d, *J*=4.5 Hz, 2H), 7.72 (m, 4H), 7.59 (m, 8H), 7.39 (d, *J*=8.4 Hz, 5H), 7.03 (d, *J*=7.8 Hz, 2H), 6.96 (d, *J*=4.5 Hz, 2H), 6.74 (d, *J*=8.1 Hz, 4H), 6.48 (m, 2H), 4.97 (s, 3H), 2.73 (s, 6H), 2.54 (s, 6H), 1.99 (s, 6H), –0.29 (s, 6H). UV/vis (CH₂Cl₂): λ_{max} [nm]=1002, 891, 634, 578, 497, 351. MALDI-TOFMS: *m/z*=1705.57 (calcd for C₉₆H₆₈N₈Re₂ [M⁺–6CO] 1706.47).

4.21. 21-Phenyl-3-methoxy *N*-confused tetrakis(*p*-tolyl)porphyrin (**25c**)

To a solution of **12a** (4.41 mg, 0.0059 mmol) in distilled THF (7 mL), 25% solution of NaOMe in MeOH (0.5 mL) was added. After stirring for 2 h, the reaction mixture was poured into aqueous NH₄Cl and CH₂Cl₂ (20 mL) was added. The organic phase was separated and dried over Na₂SO₄. The solvent was evaporated under reduced pressure and the residue was purified by column chromatography on silica gel eluted with 2% MeOH–CH₂Cl₂. The green fraction was collected and the solvent was evaporated to dryness. The residue was recrystallized from CH₂Cl₂–MeOH to afford green crystals of **25c** (1.94 mg) in 42% yield. ¹H NMR (CDCl₃): δ 8.69 (d, *J*=5.1 Hz, 1H), 8.27 (d, *J*=5.1 Hz, 2H), 8.17 (d, *J*=7.8 Hz, 2H), 8.05 (m, 4H), 7.98 (d, *J*=4.5 Hz, 1H), 7.85 (d, *J*=6.6 Hz, 2H), 7.49 (m, 10H), 5.51 (t, *J*=7.2 Hz, 1H), 5.29 (t, *J*=8.0 Hz, 2H), 3.50 (s, 3H), 3.17 (d, *J*=8.4 Hz, 2H), 2.62 (m, 12H), two inner NH signals were not observed at 25 °C. UV/vis (CH₂Cl₂): λ_{max} [nm] (log ε)=762 (3.62), 640 (3.90),

473 (4.73), 438 (4.77), 333 (4.38). MALDI-TOFMS: *m/z*=776.96 (calcd for C₅₅H₄₄N₄O [M⁺] 776.3515).

4.22. 21-Phenylethynyl-3-methoxy *N*-confused tetrakis(*p*-tolyl)porphyrin (**25d**)

To a solution of **14** (3.75 mg, 0.0049 mmol) in distilled THF (5 mL), 25% solution of NaOMe in MeOH (0.5 mL) was added. After stirring for 1 h, the reaction mixture was poured into aqueous NH₄Cl and CH₂Cl₂ (20 mL) was added. The organic phase was separated and dried over Na₂SO₄. The solvent was evaporated under reduced pressure and the residue was purified by column chromatography on silica gel eluted with 3% MeOH–CH₂Cl₂. The green fraction was collected and the solvent was evaporated to dryness. The residue was recrystallized from CH₂Cl₂–MeOH to afford green crystals of **25d** (3.70 mg) in 95% yield. ¹H NMR (CDCl₃): δ 8.78 (d, *J*=5.1 Hz, 1H), 8.66 (d, *J*=4.8 Hz, 1H), 8.43 (d, *J*=5.1 Hz, 1H), 8.32 (m, 3H), 8.21 (m, 5H), 8.02 (m, 1H), 7.70 (m, 1H), 7.52 (m, 9H), 6.37 (t, *J*=7.5 Hz, 1H), 6.07 (t, *J*=7.7 Hz, 2H), 3.78 (s, 3H), 3.46 (t, *J*=6.9 Hz, 2H), 2.67 (m, 12H), two inner NH signals were not observed at 25 °C. UV/vis (CH₂Cl₂): λ_{max} [nm] (log ε)=726 (3.80), 614 (4.06), 569 (4.01), 464 (sh, 4.84), 429 (5.03), 352 (4.71). MALDI-TOFMS: *m/z*=800.04 (calcd for C₅₇H₄₄N₄O [M⁺] 800.35).

4.23. Bis[3-methoxy *N*-confused tetrakis(*p*-tolyl)porphynyl]ethyne (**26**)

To the solution of **15** (9.8 mg, 7.2 μmol) in distilled THF (5 mL), 25% solution of NaOMe in MeOH (0.5 mL) was added. After stirring for 1 h, the reaction mixture was poured into aqueous NH₄Cl and CH₂Cl₂ (20 mL) was added. The organic phase was separated and dried over Na₂SO₄. The solvent was evaporated under reduced pressure and the residue was purified by column chromatography on silica gel eluted with 3% MeOH–CH₂Cl₂. The green fraction was collected and the solvent was evaporated to dryness. The residue was recrystallized from CH₂Cl₂–MeOH to afford green crystals of **24** (2.41 mg) in 24% yield. UV/vis (CH₂Cl₂): λ_{max} [nm]=750 (4.16), 423 (5.45), 335 (4.99). MALDI-TOFMS: *m/z*=1423.56 (calcd for C₁₀₀H₇₉N₈O₂ [M+H⁺] 1423.63).

4.24. X-ray structures

Crystallographic details are summarized in Table 2. Compound **9e**: crystals were obtained from chlorobenzene/MeOH by slow vapor-diffusion and the data crystal was a green prism of approximate dimensions 0.40×0.10×0.05 mm (C₄₅H₂₇N₄F₃Br·0.5C₆H₅Cl). Data were collected on a Rigaku R-axis diffractometer in the scan range θ≤27.5. Of the 17,287 reflections measured, 8161 were unique and 7150 had *F*₀>2σ*F*₀. Compound **12a**: crystals were obtained from CH₂Cl₂/MeOH mixed solvent and the data crystal was a green prism of approximate dimensions 0.40×0.10×0.05 mm (C₅₄H₄₀N₄). Of the 35,334 reflections measured, 9124 were unique and 5491 had *F*₀>2σ*F*₀. Compound **25a**: crystals were obtained from

Table 2
X-ray experimental details of **9e**, **12a**, and **25a**

	9e	12a	25a
Formula	C ₄₅ H ₂₆ N ₄ F ₃ Br·0.5C ₆ H ₅ Cl	C ₅₄ H ₄₀ N ₄	C ₄₅ H ₃₂ N ₄ O
FW	815.88	744.94	644.77
Color	Green	Green	Violet
Habit	Prism	Prism	Prism
Crystal system	Triclinic	Monoclinic	Monoclinic
Space group	<i>P</i> -1	<i>P</i> 2 ₁ / <i>a</i>	<i>P</i> 2 ₁ / <i>a</i>
<i>a</i> , Å	9.938(4)	14.31(3)	15.372(3)
<i>b</i> , Å	13.570(7)	14.43(2)	17.038(4)
<i>c</i> , Å	14.931(8)	19.84(3)	15.266(3)
α , °	104.33(5)	90	90
β , °	96.01(5)	103.24(15)	53.977(8)
γ , °	108.32(4)	90	90
<i>V</i> , Å ³	1815.2(16)	3988(12)	3234.5(12)
<i>Z</i>	2	4	4
Radiation (λ , Å)	Mo (0.7107)		
<i>T</i> , °C	−150.0	−150.0	−150.0
<i>D_c</i> , g/cm ³	1.493	1.240	1.324
μ , cm ^{−1}	12.28	0.073	0.080
<i>R</i> ₁ (obsd data)	0.080	0.0706	0.0996
<i>WR</i> ₂ (obsd data)	0.2126	0.1580	0.2058
GOF	1.131	1.018	1.000
Independent refs	8161	9124	7180
Observed refs	7150	5491	3061
Parameters	542	580	452

CH₂Cl₂/MeOH and the data crystal was a green prism of approximate dimensions 0.15×0.10×0.10 mm (C₄₅H₃₂N₄O). Of the 27,436 reflections measured, 7418 were unique and 3061 had $F_0 > 2\sigma F_0$. The structures were solved by direct methods and refined by full-matrix least-square procedures. The hydrogen atoms were calculated in ideal positions. Solution and structure refinement calculations for the structures were performed using the teXsan crystallographic package of Molecular Structure Corporation. Crystallographic data have been deposited at the Cambridge Crystallographic Data Centre with reference number CCDC 672463–672465 for **9e**, **12a**, and **25a**, respectively. These data can be obtained free of charge via www.ccdc.cam.ac.uk/data_request/cif.

Acknowledgements

The present work was supported by the Grant-in-Aid for Scientific Research (16350024 and 19750036) and the Global COE Program ‘Science for Future Molecular Systems’ from the Ministry of Education, Culture, Science, Sports and Technology of Japan, and PRESTO from JST, Japan. We thank Prof. Hidemitsu Uno (Ehime University) for the help of X-ray analyses and T.I. thanks JSPS for a Research Fellowship for Young Scientists.

References and notes

1. *The Porphyrin Handbook*; Kadish, K., Smith, K. M., Guillard, R., Eds.; Academic: San Diego, CA, 2000; Vols. 1–10.
2. (a) *The Porphyrin Handbook*; Kadish, K., Smith, K. M., Guillard, R., Eds.; Academic: San Diego, CA, 2000; Vol. 2; (b) Sessler, J. L.; Weghorn, S. J.

- Expanded, Contracted, and Isomeric Porphyrins*; Elsevier: Oxford, 1997; p 520; (c) Sessler, J. L.; Seidel, D. *Angew. Chem., Int. Ed.* **2003**, *42*, 5134–5175.
3. (a) Furuta, H.; Asano, T.; Ogawa, T. *J. Am. Chem. Soc.* **1994**, *116*, 767–768; (b) Chmielewski, P. J.; Latos-Grażyński, L.; Rachlewicz, K.; Głowiak, T. *Angew. Chem., Int. Ed. Engl.* **1994**, *33*, 779–781; (c) Morimoto, T.; Taniguchi, S.; Osuka, A.; Furuta, H. *Eur. J. Org. Chem.* **2005**, 3887–3890.
 4. (a) Lash, T. D. *Synlett* **1999**, 279–295; (b) Latos-Grażyński, L. *The Porphyrin Handbook*; Kadish, K., Smith, K. M., Guillard, R., Eds.; Academic: San Diego, 2000; Vol. 2, Chapter 14; (c) Furuta, H.; Maeda, H.; Osuka, A. *Chem. Commun.* **2002**, 1795–1804; (d) Harvey, J. D.; Ziegler, C. J. *Coord. Chem. Rev.* **2003**, *247*, 1–19; (e) Maeda, H.; Furuta, H. *J. Porphyrins Phthalocyanines* **2004**, *8*, 67–76; (f) Srinivasan, A.; Furuta, H. *Acc. Chem. Res.* **2005**, *38*, 10–20; (g) Chmielewski, P. J.; Latos-Grażyński, L. *Coord. Chem. Rev.* **2005**, *249*, 2510–2533; (h) Ishizuka, T.; Furuta, H. *J. Organosynth. Chem.* **2005**, *63*, 211–221; (i) Maeda, H.; Furuta, H. *Pure Appl. Chem.* **2006**, *78*, 29–44; (j) Harvey, J. D.; Ziegler, C. J. *Inorg. Biochem.* **2006**, *100*, 869–880.
 5. (a) Furuta, H.; Ishizuka, T.; Osuka, A.; Ogawa, T. *J. Am. Chem. Soc.* **1999**, *121*, 2945–2946; (b) Furuta, H.; Ishizuka, T.; Osuka, A.; Ogawa, T. *J. Am. Chem. Soc.* **2000**, *122*, 5748–5757; (c) Ishizuka, T.; Osuka, A.; Furuta, H. *Angew. Chem., Int. Ed.* **2004**, *43*, 5077–5081.
 6. (a) Toganoh, M.; Ishizuka, T.; Furuta, H. *Chem. Commun.* **2004**, 2464–2465; (b) Toganoh, M.; Ikeda, S.; Furuta, H. *Chem. Commun.* **2005**, 4589–4591; (c) Toganoh, M.; Ikeda, S.; Furuta, H. *Inorg. Chem.* **2007**, *46*, 10003–10015; (d) Toganoh, M.; Kimura, T.; Furuta, H. *Chem. Commun.* **2008**, 102–104; (e) Toganoh, M.; Fujino, K.; Ikeda, S.; Furuta, H. *Tetrahedron Lett.* **2008**, *49*, 1488–1491; (f) Młodzianowska, A.; Latos-Grażyński, L.; Sztterenber, L.; Stepień, M. *Inorg. Chem.* **2007**, *46*, 6950–6957.
 7. Maeda, H.; Osuka, A.; Furuta, H. *J. Am. Chem. Soc.* **2003**, *125*, 15690–15691.
 8. Gupta, I.; Morimoto, T.; Toganoh, M.; Furuta, H. *Angew. Chem., Int. Ed.*, in press.
 9. (a) Shin, J.-Y.; Furuta, H.; Osuka, A. *Angew. Chem., Int. Ed.* **2001**, *40*, 619–621; (b) Shin, J.-Y.; Furuta, H.; Yoza, K.; Igarashi, S.; Osuka, A. *J. Am. Chem. Soc.* **2001**, *123*, 7190–7191; (c) Shimizu, S.; Shin, J.-Y.; Furuta, H.; Ismael, R.; Osuka, A. *Angew. Chem., Int. Ed.* **2003**, *42*, 78–82; (d) Mori, S.; Shin, J.-Y.; Shimizu, S.; Ishikawa, F.; Furuta, H.; Osuka, A. *Chem.—Eur. J.* **2005**, *11*, 2417–2425; (e) Shimizu, S.; Aratani, N.; Osuka, A. *Chem.—Eur. J.* **2006**, *12*, 4909–4918.
 10. (a) Srinivasan, A.; Ishizuka, T.; Furuta, H. *Angew. Chem., Int. Ed.* **2004**, *43*, 876–879; (b) Srinivasan, A.; Ishizuka, T.; Maeda, H.; Furuta, H. *Angew. Chem., Int. Ed.* **2004**, *43*, 2951–2955.
 11. Anslyn, E. V.; Dougherty, D. A. *Expanded, Contracted, and Modern Physical Organic Chemistry*; University Science Books: Sausalito, CA, 2006; p 22.
 12. (a) Dimagno, S. G.; Lin, V. S.-Y.; Therien, M. J. *J. Am. Chem. Soc.* **1993**, *115*, 2513–2515; (b) Dimagno, S. G.; Lin, V. S.-Y.; Therien, M. J. *J. Org. Chem.* **1993**, *58*, 5983–5993; (c) Hyslop, A. G.; Kellet, M. A.; Iovine, P. M.; Therien, M. J. *J. Am. Chem. Soc.* **1998**, *120*, 12676–12677 and references therein; (d) Fletcher, J. T.; Therien, M. J. *J. Am. Chem. Soc.* **2002**, *124*, 4298–4311.
 13. Aihara, H.; Jaquinod, L.; Nurco, D. J.; Smith, K. M. *Angew. Chem., Int. Ed.* **2001**, *40*, 3439–3441.
 14. Ishizuka, T.; Yamasaki, H.; Osuka, A.; Furuta, H. *Tetrahedron* **2007**, *63*, 5137–5147.
 15. Bao, Z.; Chan, W. K.; Yu, L. *J. Am. Chem. Soc.* **1995**, *117*, 12426–12435.
 16. Stepień, M.; Latos-Grażyński, L. *Org. Lett.* **2003**, *5*, 3379–3381.
 17. (a) Osuka, A.; Shimidzu, H. *Angew. Chem., Int. Ed.* **1997**, *36*, 135–137; (b) Aratani, N.; Osuka, A.; Kim, Y.-H.; Jeong, D.-H.; Kim, D. *Angew. Chem., Int. Ed.* **2000**, *39*, 1458–1462.